

# Friction Stir Surface Processing of Al 6061 Alloy: Role of Surface Alloying with Copper and Heat-Treatment

Kaustubh M. Mane<sup>1</sup> · Santosh S. Hosmani<sup>2</sup>

Received: 8 June 2017 / Accepted: 12 January 2018 / Published online: 27 January 2018  
© The Indian Institute of Metals - IIM 2018

**Abstract** The current paper focuses on enhancing the surface hardness of the heat-treatable Al-alloy using the combined approach of thermal-spray, friction stir surface processing (FSSP) and heat-treatment. Copper powder was thermal-sprayed in the surface groove of Al 6061 alloy specimens followed by FSSP. Defect-free stirred zone was observed at lower transverse speed of 10 mm/min. The width of the hardness profiles across the stirred zone was increased with increase in the rotational speed of the tool. Grain refining was observed in the stirred zone due to the FSSP. In post-FSSP T6 heat-treatment, aging kinetics in the non-surface-alloyed specimen was accelerated due to the FSSP. Precipitation of Al<sub>2</sub>Cu phase was observed in the stirred zone. Copper-alloying and post-FSSP heat-treatment were effective in enhancing the surface hardness (about 39% improvement in the surface hardness was observed).

**Keywords** Aluminum-alloys · Hardness · Microstructure · Surface treatment · Friction stir

## 1 Introduction

In many engineering applications, there is a quest for weight reduction of the components to enhance the efficiency and fuel economy. It is important that the critical parameters, like strength, surface hardness etc., should not be compromised while reducing the weight of the components. Aluminum alloys are the attractive engineering material due to their lower density than steels. However, the aluminium alloys are soft and have poor tribological properties. The approach of surface compositing can help in achieving the good surface hardness and wear resistance without compromising the original properties of the substrate [1]. Surface metal matrix composites (SMMC) can be obtained by introducing hard particles in the surface of Al alloys [1]. Conventional surface modification techniques include laser melt treatment, plasma spraying, and liquid phase processing techniques etc. These processes are done at elevated temperatures, and there is the possibility of formation of unwanted brittle phases during solidification (due to the reaction between the reinforcement and the metal-matrix). Apart from this, many parameters must be controlled precisely to obtain the desired microstructure of the surface layer. In case of the hybrid reinforcements, agglomeration leads to the inhomogeneous distribution of the reinforcement (which is the typical issue of fusion surface processing techniques) [2, 3]. However, these problems can be eliminated if the surface compositing is done at a temperature below the melting point of the substrate. Friction stir processing is a technique which processes the surface in a solid state. This process has the capability to modify the microstructure of the metals. Recently, friction stir processing is applied for compositing the metal surface [3–6]. The friction stir processing technique is developed on the concept of friction stir welding

✉ Santosh S. Hosmani  
sshosmani@iiti.ac.in

Kaustubh M. Mane  
kaustubh290888@gmail.com

<sup>1</sup> Department of Metallurgy and Materials Science, College of Engineering, Pune 411005, Maharashtra, India

<sup>2</sup> Metallurgy Engineering and Materials Science, Indian Institute of Technology Indore, Khandwa Road, Simrol, Indore 453552, Madhya Pradesh, India

(FSW) [2]. Stirring action and frictional heat produced by the non-consumable rotating tool can be used to distribute the reinforced particles uniformly on the surface of Al alloys [2]. Material mixing in the stirred zone is considerably dependent on the geometry of the rotating tool [7]. The triangular and square pin tools produce a pulsating stirring action in the flowing material (due to their flat faces). However, there is no such pulsating action in case of cylindrical, tapered and threaded pin profiles [7].

Properties of the alloy can be manipulated by varying the friction stir process-parameters [8, 9]. An optimum combination of transverse speed and a rotational speed of the tool is essential to achieve the maximum hardness of the surface composites [9]. Friction stir processing can enhance the hardness of the stirred zone due to the grain refinement [5]. Hoffman et al. [10] and Darras et al. [11] had obtained nanometer sized grains by modifying the friction stir technique, where they conducted the process by keeping the substrate underwater rather than in air. Morisada et al. [12] had obtained grain refinement up to nanometer scale by dispersing the fullerene in the Al alloy.

Aluminium alloys have wide applications in the aircraft industries. Most of the recent literature related to the friction stir surface processing techniques focuses on the role of process parameters and the dispersion of hard ceramic particles in the surface layer of non-ferrous alloys [13–20]. Current paper attempts the enhancement of surface-hardness of the heat-treatable Al-alloy using the combined approach of thermal-spray, friction stir surface process (FSSP) and age hardening treatment. In this work, copper was mechanically mixed on the surface of Al 6061 alloy using thermal-spray and friction stir surface process (FSSP), and subsequently, age hardened to form precipitates of hard phase. Effect of FSSP parameters and post-FSSP heat-treatment on the microstructure and hardness has been studied.

## 2 Materials and Methods

In the current work, Al 6061 was selected as the substrate for friction stir surface processing (FSSP). This alloy is a heat treatable grade of Al alloys. The chemical composition of this alloy is shown in Table 1. As received hardness

of this alloy was 107 HV<sub>0.1</sub>. Specimens of size 100 mm (length) × 30 mm (width) × 8 mm (thick) were used for the experiments.

Two different geometries of the tool were used for FSSP: (1) square pin and (2) conical pin tools. Shoulder diameter was 15 mm for both the tools. The dimension of square pin sides was 6 mm and the length of the pin was 1 mm. The conical pin had a maximum diameter of 7 mm near the shoulder and minimum diameter of 3 mm at the tip. Length of the conical pin was 4.5 mm. The shank diameter was 12 mm for both the tools. Shank helped to hold the tool in collet during processing on the CNC (computer numerical control) machine. H13 tool steel was used to manufacture the tools. Before using the tools for FSSP, they were heat-treated (austenitizing at 1030 °C → quenching in oil → tempering at 580 °C). Heat-treated tools were rough ground and polished to obtain the smooth surface finish.

FSSP was done on the Premier vertical milling machine (model: PVM 40). This machine had a FANUC CNC system. All the degrees of freedom of the specimen during friction stir processing were restricted using the fixture. During FSSP, traversing and rotating tool must tilt towards the trailing side of the traversing direction to ensure proper forging action on the specimen and mixing/stirring of plastic material. The angle thus created by the tool with the vertical direction is called the ‘tilt angle’. Generally, this tilt angle could be provided by tilting the spindle of the machine. As this facility was not available in the machine used in this work, an alternative arrangement was made to provide the tilt angle. A plate with 3° gradient was designed for this purpose. Al 6061 specimen was kept on this gradient plate and clamped to the fixture plate. The CNC programming was done such that the tool traversed horizontally and vertically simultaneously (to move along the gradient plate), and thus, maintained the constant plunge depth throughout the scan.

The rotational speed of the tool for FSSP was 1300, 2000, and 3000 rpm. The transverse speed of the tools was varied from 10 to 50 mm/min. For square pin tool, the plunge depth was kept constant at 1.2 mm throughout the experiments. The temperature of the stirred zone during the FSSP was measured using a laser pyrometer and thermocouple.

**Table 1** Chemical composition of as received Al 6061 alloy

Element	Al	Cu	Cr	Ti	Mn	Si	Mg	Fe	Zn
Composition (wt%)	97.7	0.18	0.049	0.065	0.07	0.66	0.85	0.34	0.06

The material to be surface-alloyed (Cu in the current work) was deposited on the alloy substrate. In case of FSSP, the shoulder plunges into the substrate along with the rotating pin, and therefore, the deposition technique should be such that the deposited material should remain in place without delamination. Thermal-spraying was used to deposit Cu on the Al 6061 specimen. A groove was cut on the substrate to deposit Cu. Grooves of two different widths (3 mm and 5 mm) and 1 mm depth were cut using end mill cutter. Before thermal-spraying, the surface of the substrate was roughened using grit blasting. Chilled-iron grits of size 0.4–0.8 mm were used for grit blasting. Grits were accelerated towards the substrate using compressed air at 5 bar pressure. The grit blasting was done for 10 s.

Copper powder of size 40–90  $\mu\text{m}$  (400–170 mesh size) was used for the thermal-spraying. Average particle size was about 65  $\mu\text{m}$ . SEM micrograph of the Cu powder used in this study is shown in Fig. 1. Chemical composition of the powder is as follows: 99.6% Cu, 0.005% Sb, 0.0002% As, 0.05% Pb, 0.005% Fe, and 0.005% Mn. It was sprayed on the grit-blasted surface using powder flame gun (make: MEC, Jodhpur, India), where the oxy-acetylene flame was used. The flow rate of oxygen and acetylene was kept at 30 ml/min each. Molten droplets of Cu were accelerated towards the substrate using compressed air at 5 bar pressure. Thermal-spraying was done until the groove was filled completely with copper.

Thermally sprayed specimens were subjected to the stress relieving heat-treatment, before FSSP, at 420  $^{\circ}\text{C}$  for 2 h followed by furnace-cooling. FSSP of such Cu sprayed surface was done as per the procedure described above.

FSSPed specimens (with and without copper surface-alloying) were subjected to T6 heat-treatment. T6 heat-

treatment involved the following three steps: solutionizing, quenching and aging. Solutionizing was done at 530  $^{\circ}\text{C}$  for 2 h (followed by water quenching). Artificial aging was done at 140 and 180  $^{\circ}\text{C}$  for various durations in the range of 2–22 h.

Microstructures of the polished and etched (by using Keller's reagent) specimens were obtained using optical-microscope (model: Zeiss Axiovert 40 MAT). The hardness of the specimens was obtained using microhardness tester (model: Future Tech FM-700). Microhardness measurements were done using 100 g load and 10 s dwell-time. The microhardness profiles were recorded at the two different locations of FSSPed specimens—(1) on the surface across the stirred zone, and (2) across the cross-section from the center of the stirred zone. Phase analysis was done using X-ray diffraction (XRD) technique (model: Bruker AXS), where Cu radiation ( $\lambda = 1.5405 \text{ \AA}$ ) was used. XRD peaks were identified using XPERT-PRO XRD software.

### 3 Results and Discussion

#### 3.1 Friction Stir Surface Processing (FSSP) of Al 6061 Alloy

##### 3.1.1 Effect of FSSP Parameters on Macrostructure

FSSP is done using different pin profiles at different rotational speeds of the tools. Some defects are observed in the cross-section when FSSP is done using certain process-parameters (Fig. 2). When square pin tool is used at 1300 rpm, a tunneling defect is observed at the bottom of the stirred zone/nugget zone (Fig. 2a). In this defect, a large cavity is left across the length of the FSSPed specimen. However, this defect is not observed at higher rotational speed (3000 rpm) of the same square pin tool (Fig. 2b). As the rotational speed of the tool is increased, material mixing becomes more uniform and the tunneling defect is not observed. In case of the conical pin tool, such defect is not observed even at lower rotational speed (Fig. 2c). This may be attributed to the absence of pulsating action within the stirred zone when conical pin tool is used [7, 8].

The transverse speed of the rotating square pin tool is varied (keeping the constant rotational speed of 3000 rpm) to check the feasibility of FSSP (Fig. 3). It is observed that FSSP can be done successfully at lower transverse speed rather than at higher speed. Increase in the traverse speed results in the poor mixing of the material, and therefore, the cavities and wide cracks are formed in the stirred zone. The transverse speed of 10 mm/min is found to be effective in obtaining the defect-free stirred zone (Fig. 3a) and hence, it is used throughout the experiments.

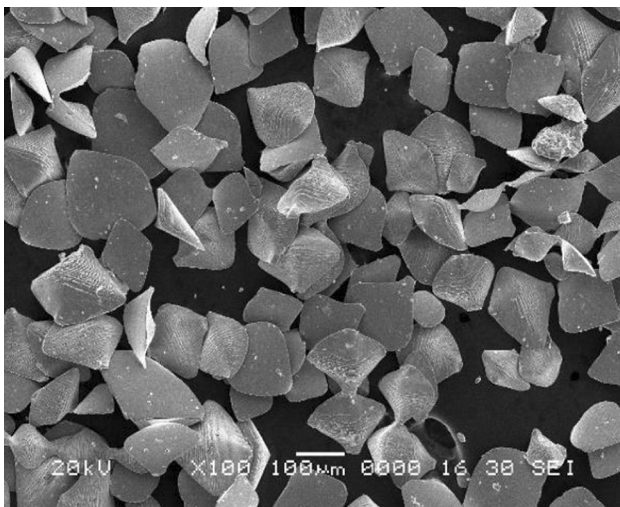


**Fig. 1** SEM micrograph of Cu powder used in the current work

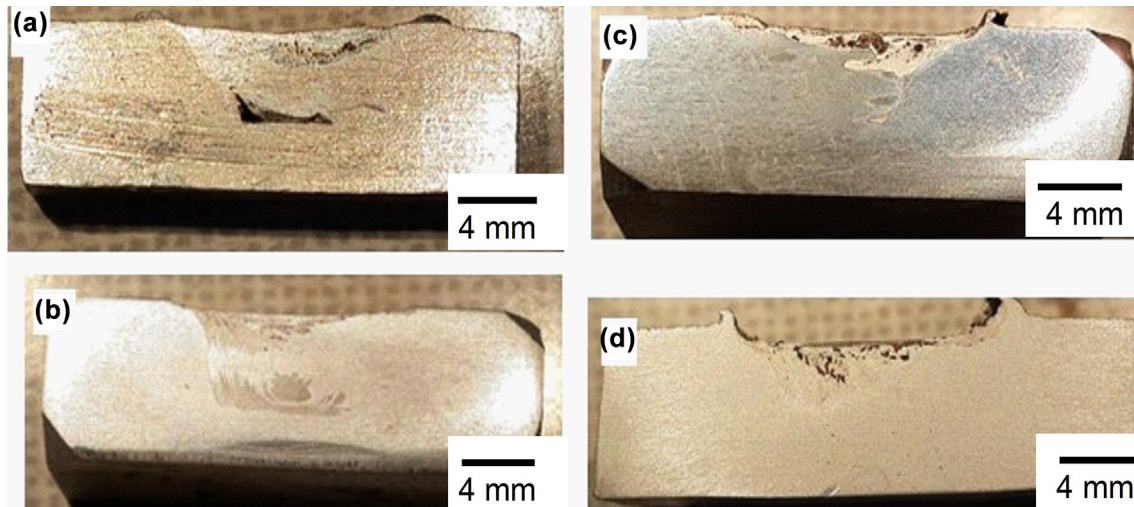


**Fig. 2** Cross-sectional macrographs of FSSPed specimens by using **a** square pin at 1300 rpm, **b** square pin at 3000 rpm, **c** conical pin at 1300 rpm, **d** conical pin at 3000 rpm

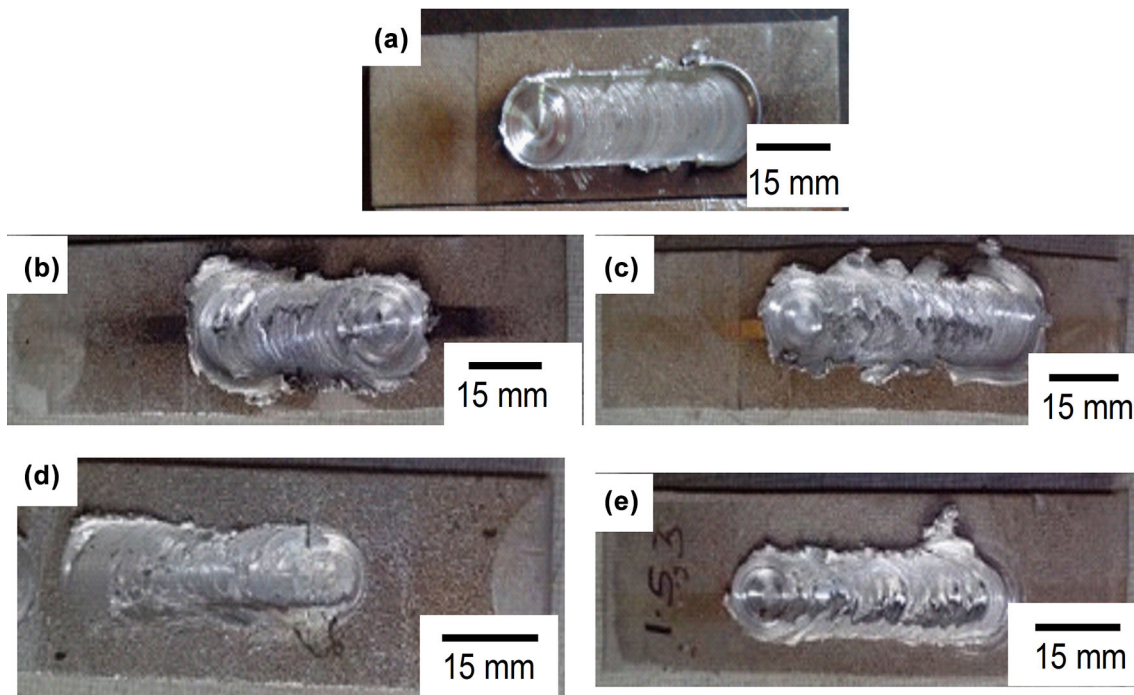


**Fig. 3** Top view of FSSPed specimens by using square pin tool at various transverse speeds: **a** 10, **b** 20, **c** 30, **d** 40 and **e** 50 mm/min

### 3.1.2 Role of FSSP on Ageing Kinetics

Friction stir surface processing (FSSP) is performed on the solutionized Al 6061 alloy using square pin tool with 1 mm pin length (2000 rpm rotational speed and 10 mm/min traverse speed). Figure 4 shows the macrograph and micrographs of the cross-section of the FSSPed region. Stirred zone, which is formed near to the surface, is visible in the macrograph. Figure 4a–d shows the

micrographs of various areas that are marked on the macrograph. Material flow patterns formed during FSSP are observed in Fig. 4a–c. Figure 4d shows the microstructure within the nugget region (stirred zone). Refined grains of size less than 10  $\mu\text{m}$  are observed in the stirred zone (grain size of non-FSSPed alloys is about 60–70  $\mu\text{m}$ ).

Temperature profiles of the stirred zone during FSSP of Al 6061 alloy are shown in Fig. 5. During FSSP, the

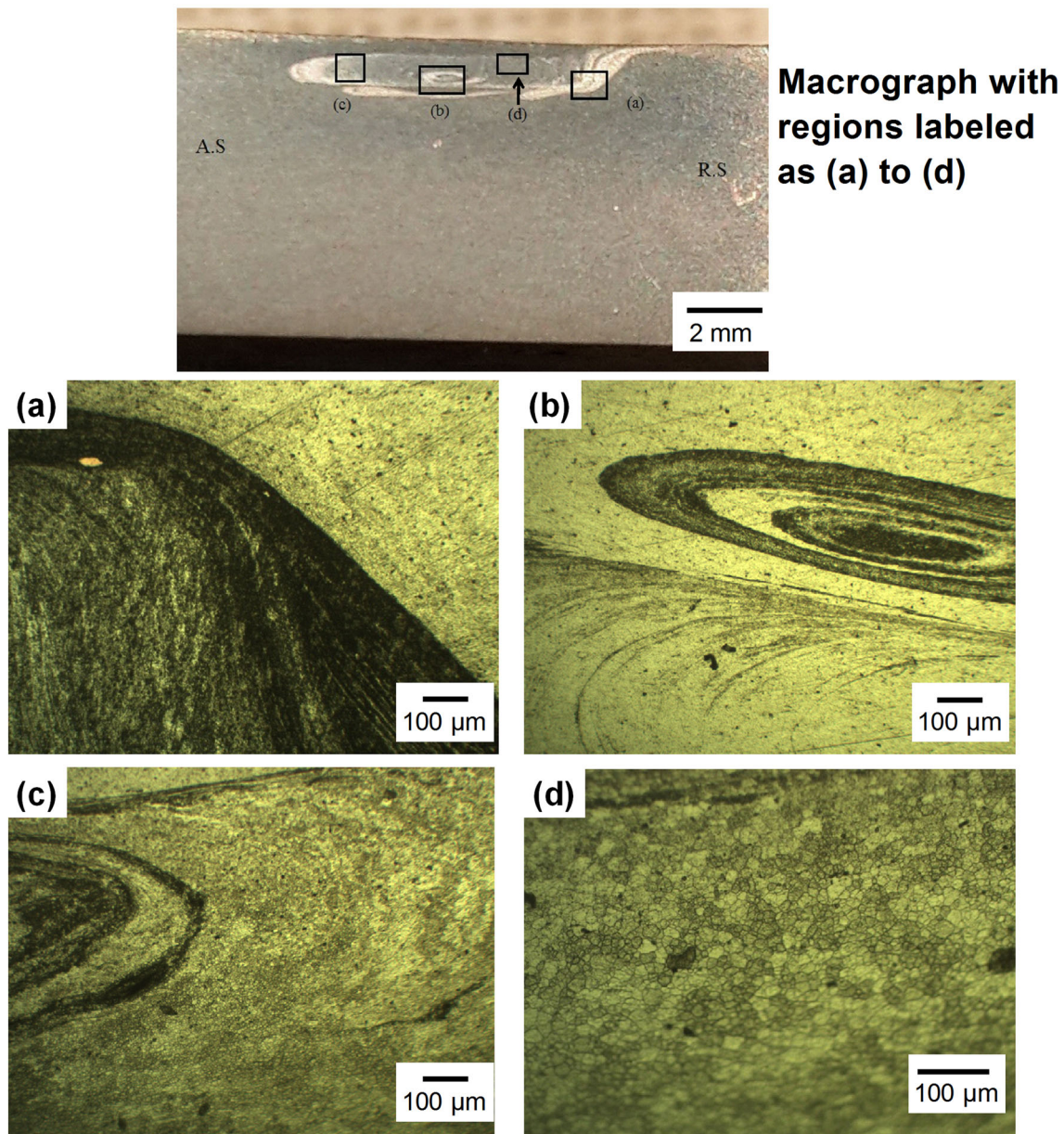


**Fig. 4** Top of the figure shows the macrograph of the cross-section of the FSSPed region of solutionized Al 6061 alloy. **a–d** Micrographs of the various areas marked and labeled on the macrograph

peak temperature of the stirred zone is about 350 °C. The peak temperature measured by the thermocouple is somewhat lower than that measured by laser pyrometer. This is so because thermocouple is placed in the hole drilled adjacent to the stirred zone. However, the laser pyrometer measures the temperature directly in the stirred zone. This temperature rise combined with the severe plastic deformation can start the process of dynamic aging during FSSP. Therefore, the grain refinement (as mentioned above: see also Fig. 4d) and

the dynamic aging (temperature rise of the stirred zone during FSSP is above 0.5  $T_m$ , where  $T_m$  is melting point in Kelvin) are responsible for the higher hardness of the stirred zone of FSSPed specimen as compared to the solutionized non-FSSPed specimen (Table 2) [21].

Specimens of the solutionized FSSPed and solutionized non-FSSPed Al 6061 alloy are aged at 140 and 180 °C for various durations. Microhardness of the surface of aged specimens (at the center of the stirred zone) is shown in Fig. 6. Maximum hardness achieved through aging is about

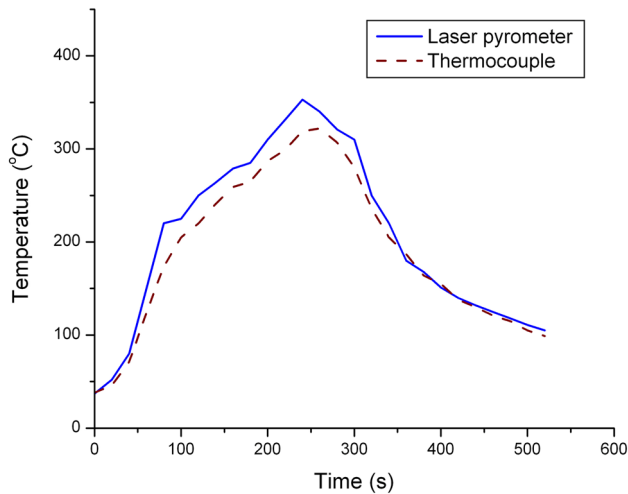


**Fig. 5** Temperature profile of the stirred zone during FSSP of Al 6061 alloy. Temperatures are measured using laser pyrometer and thermocouple

115 HV<sub>0.1</sub>. At 140 °C aging temperature, the peak hardness is achieved within 8 h for the specimen FSSPed before aging, and the specimen without FSSP takes 18 h to attain the peak hardness. In case of 180 °C aging temperature, peak hardness is achieved within 3 h for the specimen FSSPed before aging, however, it takes 12 h for the non-FSSPed specimen. These results suggest that the higher temperature and FSSP accelerate the aging kinetics.

The concept of precipitation hardening is responsible for the rise in hardness during aging [22, 23]. The well-known precipitate in T6 heat treated Al 6061 alloy is Mg<sub>2</sub>Si [24]. Dislocations, grain-boundaries (as mentioned above, FSSP causes the grain refinement and therefore, the grain-boundary area per unit volume is more for FSSPed specimen than non-FSSPed specimen), and internal stress fields are the potential nucleation sites for the precipitation in FSSPed specimens. As a result, aging kinetics is accelerated considerably for the FSSPed specimen.

## 3.2 Surface Alloying of Al 6061 with Copper by Using FSSP

### 3.2.1 Optimisation of the Aging Time

Al 6061 alloy specimens are thermally sprayed with copper powder, and FSSP is done subsequently (using square pin tool at 3000 rpm rotational speed and 10 mm/min traverse speed). The FSSPed specimens are subjected to the T6 heat treatment so that precipitation can occur in the non-FSSPed substrate (i.e. in the core) as well as in the copper alloyed surface layer. To optimise the aging time, solutionized specimens are aged for various durations. Figure 7 shows the microhardness (at the center of the stirred zone) versus aging time at 180 °C. The maximum hardness of about 156 HV<sub>0.1</sub> is obtained after 12 h of aging.

The X-ray diffraction (XRD) patterns recorded from the surface of as-received Al 6061 alloy, stirred zone of FSSPed specimen without surface-alloying, and T6 heat-treated stirred zone of the Cu surface-alloyed specimen (in subsequent text, this specimen is designated as ‘Al 6061-Cu’, where ‘-Cu’ indicates Cu surface alloying) are shown in Fig. 8. Only aluminium peaks are observed for the as-received and FSSPed Al 6061 specimens. Usually, Al 6061 alloy contain Mg<sub>2</sub>Si precipitates [24]. But, the amount of Cu, Mg, and Si in this alloy is very low. Therefore, the peaks corresponding to Mg<sub>2</sub>Si precipitates are not observed in the XRD patterns. However, FSSPed Al 6061-Cu alloy shows the peaks corresponding to aluminium and Al<sub>2</sub>Cu.

### 3.2.2 Microstructural Changes

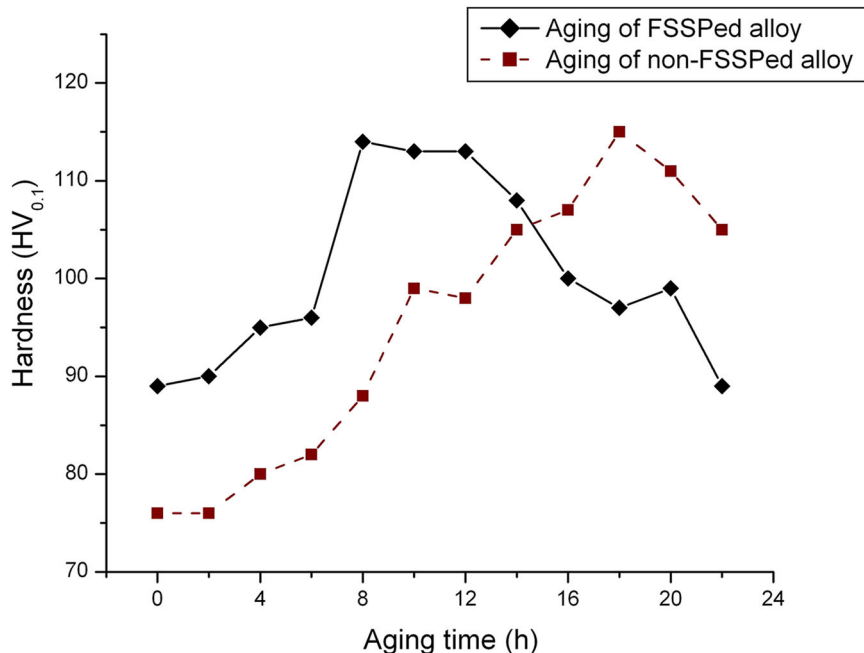
Figure 9a–d shows the top and cross-sectional views of the thermally sprayed Al 6061-Cu specimens. Figure 9e shows the macrograph of the cross-section of FSSPed (using square pin tool with 1 mm pin length at 3000 rpm rotational speed and 10 mm/min traverse speed) plus T6 heat-treated Al 6061-Cu specimen. FSSP is the thermo-

**Table 2** Surface hardness of the specimens at various conditions studied in this work

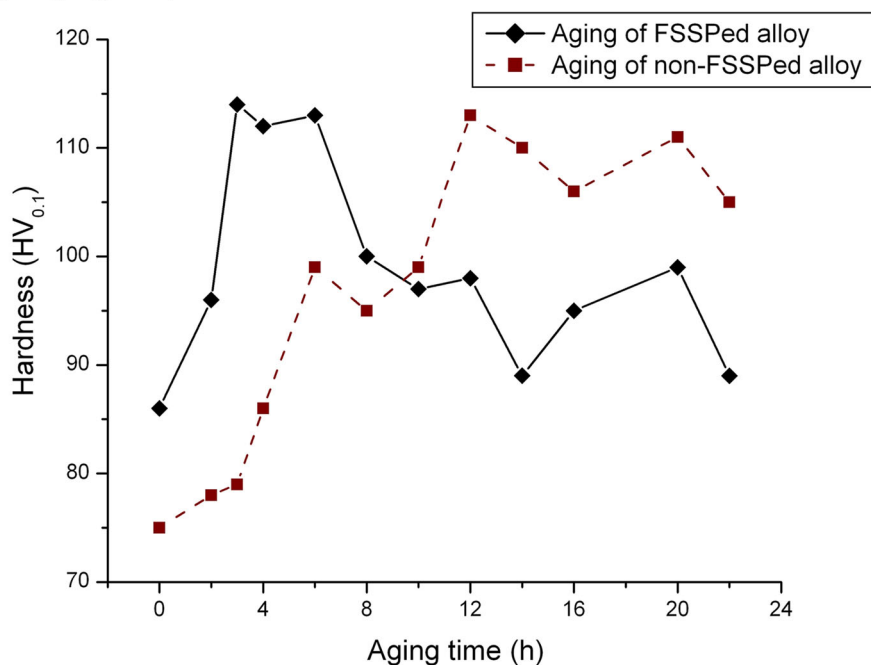
Condition of the specimen	Maximum surface hardness (HV <sub>0.1</sub> )
Non-FSSPed Al 6061 (solutionized)	76
FSSPed Al 6061	89
Aging of non-FSSPed Al 6061 ( <i>T</i> :140 °C, <i>t</i> : 18 h or <i>T</i> : 180 °C, <i>t</i> : 12 h)	115
Aging of FSSPed Al 6061 ( <i>T</i> :140 °C, <i>t</i> : 8 h or <i>T</i> : 180 °C, <i>t</i> : 3 h)	115
FSSPed Al 6061-Cu	80
Aging of FSSPed Al 6061 ( <i>T</i> :180 °C, <i>t</i> : 12 h)	160

**Fig. 6** Hardness versus aging time at **a** 140 and **b** 180 °C for FSSPed and non-FSSPed Al 6061 specimens

**(a) Aging temperature: 140 °C**



**(b) Aging temperature: 180 °C**



mechanical process, where the specimen is subjected to severe plastic deformation, and frictional heating causes the rise in temperature (see the last paragraph of this subsection). Because of this, various zones are formed in the FSSPed specimen (see the marked regions in Fig. 9e). These zones are: (1) base metal (B.M.), (2) thermo-

mechanically affected zone (T.M.Z.) and (3) stirred zone (S.Z.). The characteristics of these zones during FSSP are described in Table 3. Micrographs of different zones of the cross-section are shown in Fig. 10. Considerable grain refinement is observed in the stirred zone as compared to the base metal (Figs. 10a, b vs 10e–f). Stirred zone shows

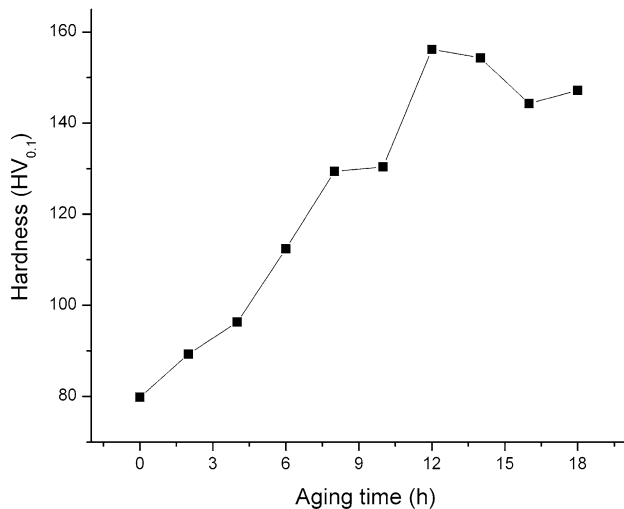


**Fig. 7** Hardness versus aging time at 180 °C for FSSPed Al 6061-Cu specimens

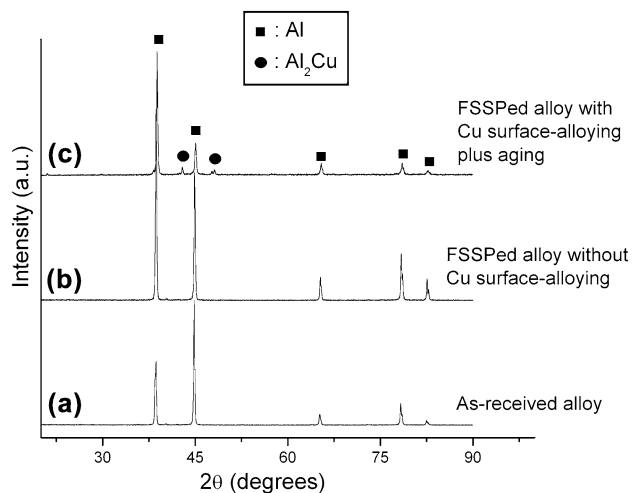


**Fig. 8** X-ray diffraction (XRD) patterns recorded from the surface of **a** as-received Al 6061 alloy, **b** stirred zone of the FSSPed specimen (without Cu surface-alloying), and **c** FSSPed and age hardened Al 6061-Cu specimen

equiaxed grains of size less than 10  $\mu\text{m}$ . As mentioned above, the grain refinement is attributed to the dynamic recrystallization [21] within the stirred zone during FSSP. Material flow induced by the severe plastic deformation causes uniform mixing of copper within the stirred zone. In the thermo-mechanically affected zone, minute elongation/deformation of the grains is observed (Fig. 10c, d). Shearing type of action in the adjacent stirred zone leads to the elongation of grains in the direction of stirring force.

Figure 11 shows the change in temperature within the stirred zone during FSSP (using square and conical pin tools at 3000 rpm rotational speed and 10 mm/min traverse speed) of Al 6061-Cu specimens. The square and conical

pin tools show the peak temperature of 470 and 415 °C in the stirred zone respectively. Higher peak temperature for the square pin tool (even though it has the shorter pin-length) confirms the more frictional heating and vigorous material-mixing caused by its pulsating action [7].

### 3.2.3 Microhardness

Microhardness measurements are done at various locations of the stirred zone to understand the behavior of FSSP plus T6 heat-treatment of Al 6061-Cu alloy. Figure 12 shows the hardness profiles recorded from the following two locations—(1) on the surface across the stirred zone, and (2) along the cross-section at the center of the stirred zone. Before FSSP of the specimens, thermal spraying of Cu is done in the groove (3 mm width and 1 mm deep). Hardness in the stirred zone is considerably higher than the base metal. Uniform hardness across the stirred zone (especially, for square pin tool) suggests the uniform mixing of Cu within the stirred zone, which is precipitation-hardened during subsequent T6 heat-treatment. Along the cross-section at the center of the stirred zone, continuous decrease in the hardness is observed from the surface to the core of the specimen. This behavior is associated with the decrease in copper content from the surface to core. The thickness of the hardened layer is about 1 mm. Square pin tool causes the marginally lower depth of the hardened layer along the cross-section of the FSSPed layer (Fig. 12c, e, g) due to the shorter pin-length.

In case of the specimens, without surface alloying with Cu, maximum surface hardness achievable after aging is 115 HV<sub>0.1</sub> (Table 2). However, for Cu surface-alloyed specimens, maximum surface hardness achievable after aging is 156 HV<sub>0.1</sub> (Table 2). This confirms that the surface alloying with Cu helps in enhancing the surface hardness of the alloy (due to the precipitation of Al<sub>2</sub>Cu phase—see also Fig. 8).

When the conical pin tool is used for FSSP, a sharp drop in the hardness is observed in the retreating side (R.S.) (see Fig. 12a, d, f). This drop in the hardness is observed at all rotational speeds. Metallographic investigation shows the difference in the size of microhardness indentations (under the same load, i.e. 100 g) obtained on the mixed region of the stirred zone and on the region neighboring to the stirred zone (which is designated as ‘unmixed region’) (Fig. 12b). This drop in hardness is due to the copper which is not mixed with the matrix in this region (i.e. Cu is agglomerated without dissolving and precipitating during heat-treatment). However, such region is not observed when square pin tool is used for FSSP (Fig. 12). Hardness profiles across the stirred zone are more uniform and wider for the specimens FSSPed using square pin tool than the conical pin tool (Fig. 12a, d, f). The possible reason for



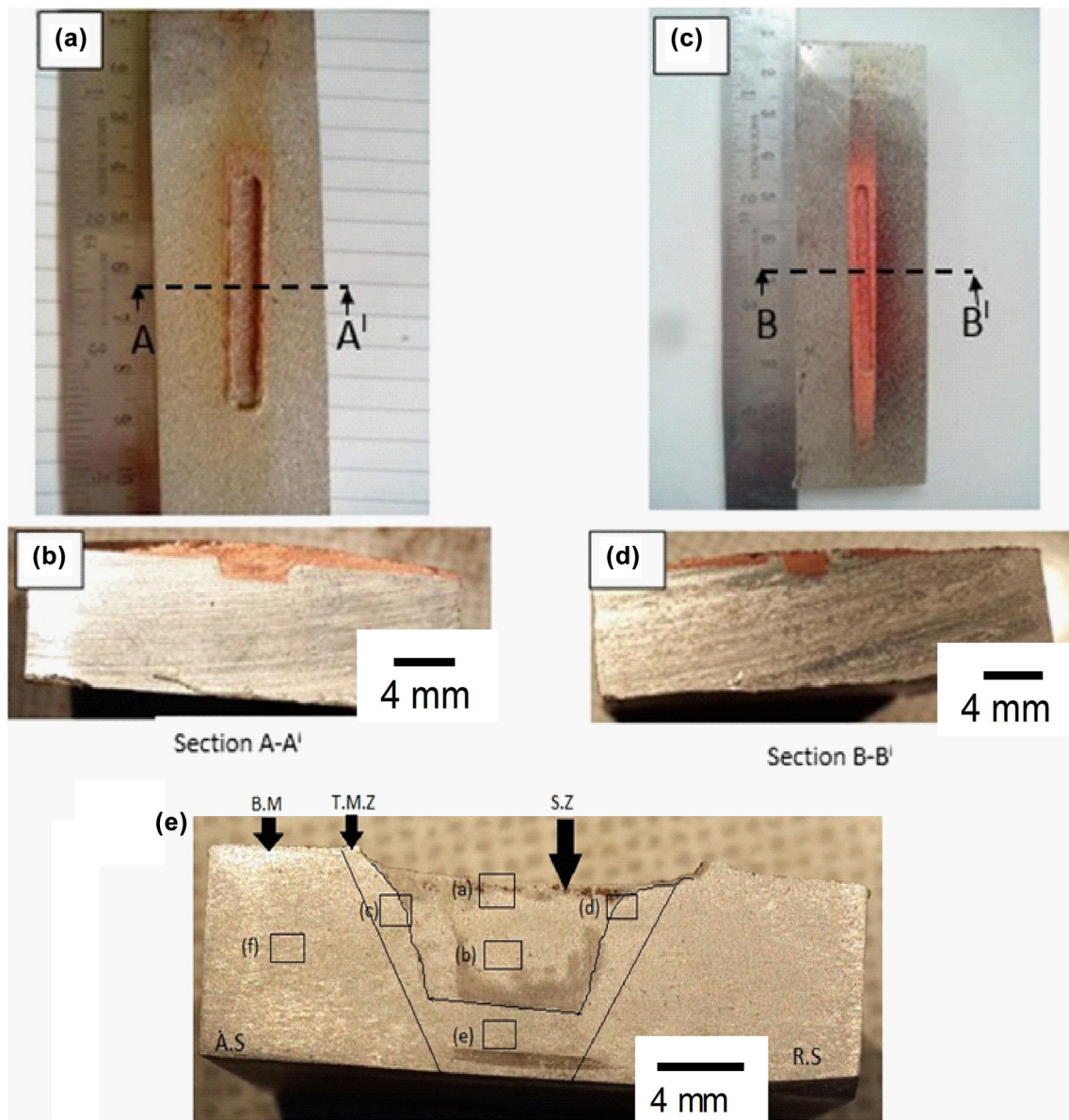


**Fig. 9** **a** Top and **b** cross-sectional view of Al 6061 specimen (non-FSSPed), where the specimen is thermally sprayed with Cu on 5 mm width groove. **c** Top and **d** cross-sectional view of Al 6061 specimen (non-FSSPed), where the specimen is thermally sprayed with Cu on 3 mm width groove. **e** Macrograph of the cross-section of FSSPed and age hardened Al 6061-Cu specimen

**Table 3** Characteristics of the various zones, which are shown in Fig. 8e, during FSSP

Zone	Plastic deformation	Temperature (measured by laser pyrometer)
Stirred zone (S.Z.)	High	High (300–475 °C)
Thermo-mechanically affected zone (T.M.Z.)	Low	Medium (100–300 °C)
Base metal (B.M.)	No	Low (room temperature—100 °C)

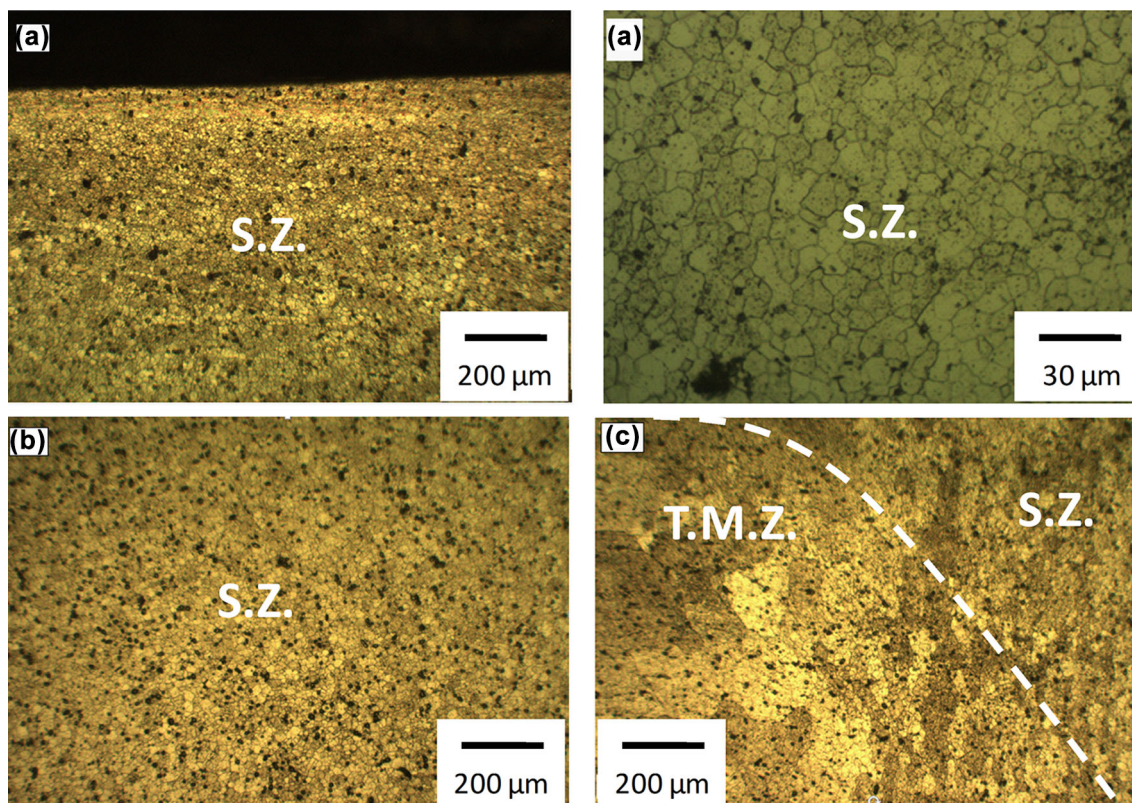


**Fig. 10** Microstructures of the cross-section of FSSPed and age hardened Al 6061-Cu specimen. These microstructures correspond to the different areas of the cross-section that are marked and labeled in Fig. 9e

these differences in FSSP behavior of Al 6061-Cu alloy using square and conical pin tools are as follows [5, 7]. Square pin tool has flat faces. Such pin profile is associated with the eccentricity, which helps to pass the incompressible material around the pin profile. Dynamic orbit is related to the eccentricity of the rotating object. The path for the flow of plasticized material from the leading edge to the trailing edge of the rotating tool depends on the relationship between the dynamic volume and static volume (i.e. ratio of the swept volume during rotation to the volume of the pin itself) [25]. This ratio is a significant factor in reducing the defects and improving the material mixing. This ratio is more for the square pin tool than the conical pin tool (it is 1.56 for square pin tool and 1.09 for conical pin tool) [5]. The reason for this is the insufficient heat input and poor flow of the plasticized metal when the conical pin tool is used. Another issue with conical pin tool is the absence of pulsating action which, otherwise, is present in the case of square pin tool (here, the pulsating stirring action in the flowing material is due to its flat

faces). Due to the combined action of the absence of both, eccentricity and pulsating stirring action, and insufficient heat input, the material mixing is poor for the conical pin tool. Therefore, Cu in the grooves is not mixed uniformly with the alloy matrix by the conical pin tool, and it remains unmixed in the retreating side.

Microhardness profiles across the stirred zone (Fig. 12a, d, f) are extended more towards the retreating side (R.S.) than the advancing side (A.S.) because the tool rotation (which is clockwise in this case) tends to move the material from the advancing side towards the retreating side (Cu is mixed comparatively wider in the retreating side).

The width of the hardness profile across the stirred zone increases considerably as the rotational speed of square pin tool is increased (Figs. 12a, d, f, 13). At the higher rotational speed of the tool, material mixing is easier due to more plastic nature (caused by more heat input) of the stirred zone, and Cu is mixed over the wider region.

Figure 13 shows the microhardness profiles across the stirred zone and along the cross-section (at the center) of

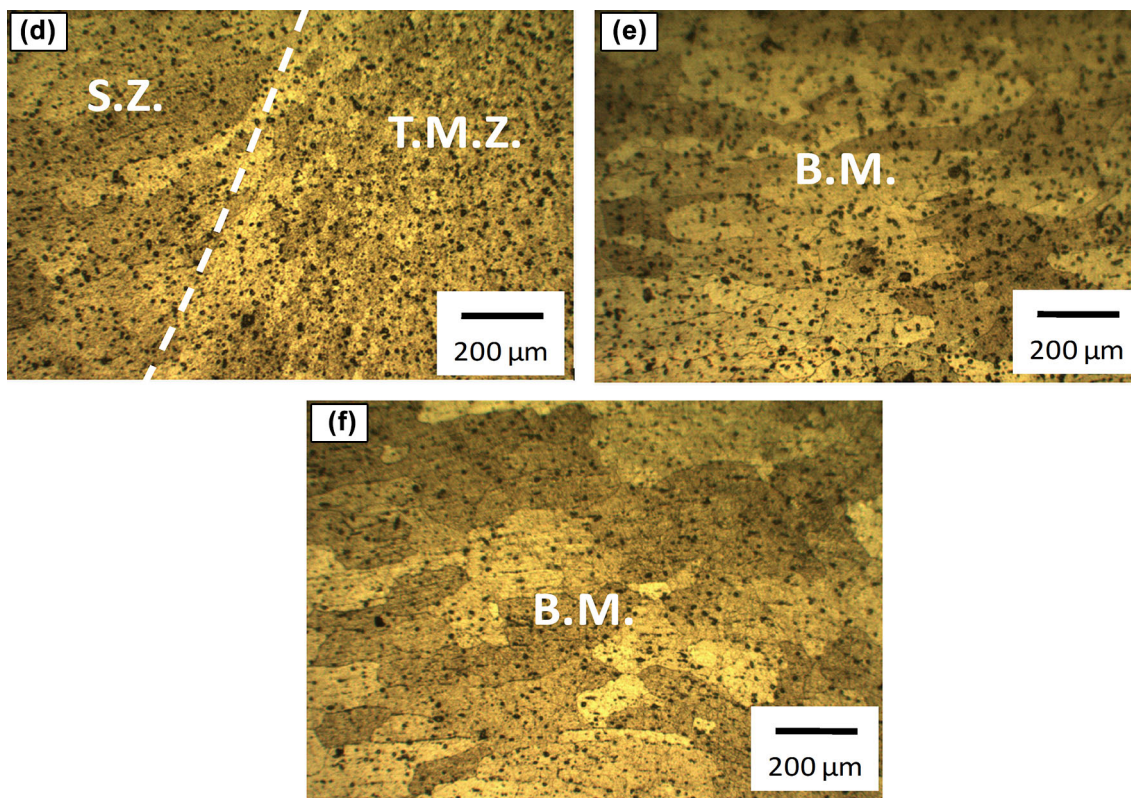


Fig. 10 continued

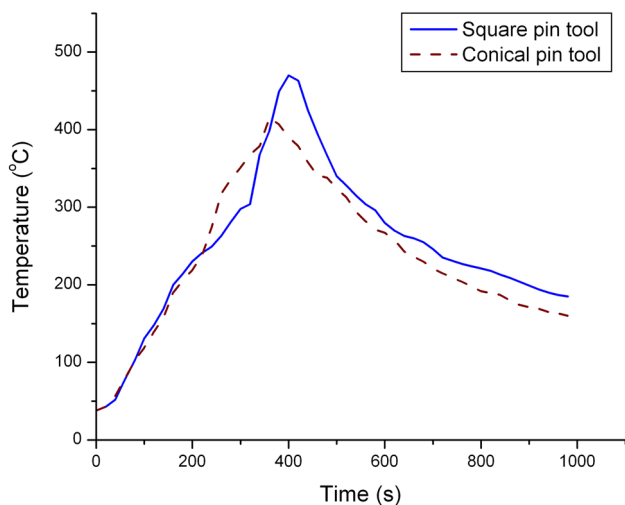


Fig. 11 Change in temperature within the stirred zone during FSSP of Al 6061-Cu specimens using both square and conical pin tools at 3000 rpm and 10 mm/min traverse speed. Temperatures are measured using laser pyrometer

the stirred zone of Al 6061-Cu specimens, where copper spraying is done in 5 mm width and 1 mm deep groove. These specimens are FSSPed by using square pin tool at

10 mm/min transverse speed and various rotational speeds. Hardness results are not affected much by changing the width of the groove from 3 to 5 mm (Figs. 13 vs 12).

### 3.2.4 Mechanism Responsible for Increased Hardness in the Stirred Zone

Al 6061 alloy is a heat-treatable grade of Al-alloys. Age hardening of this alloy causes the precipitation of  $Mg_2Si$  precipitates [24]. About 51% rise in the hardness, in comparison with the solutionized condition, is possible after aging of non-surface-alloyed Al 6061 alloy (Table 2). FSSP causes the grain refinement and therefore, the grain-boundary area per unit volume is more for FSSPed specimen than the non-FSSPed specimen. Dislocations, grain-boundaries, and internal stress fields are responsible for the enhanced aging kinetics. However, FSSP does not help in enhancing the surface hardness of the age hardened alloy.

Surface alloying with Cu (thermal spray plus FSSP) is a promising approach to make the surface harder than the usually achievable hardness of the age hardened Al 6061 alloy. FSSP technique helps in uniform mixing of Cu in the surface of the alloy. Surface hardness is 39% higher than

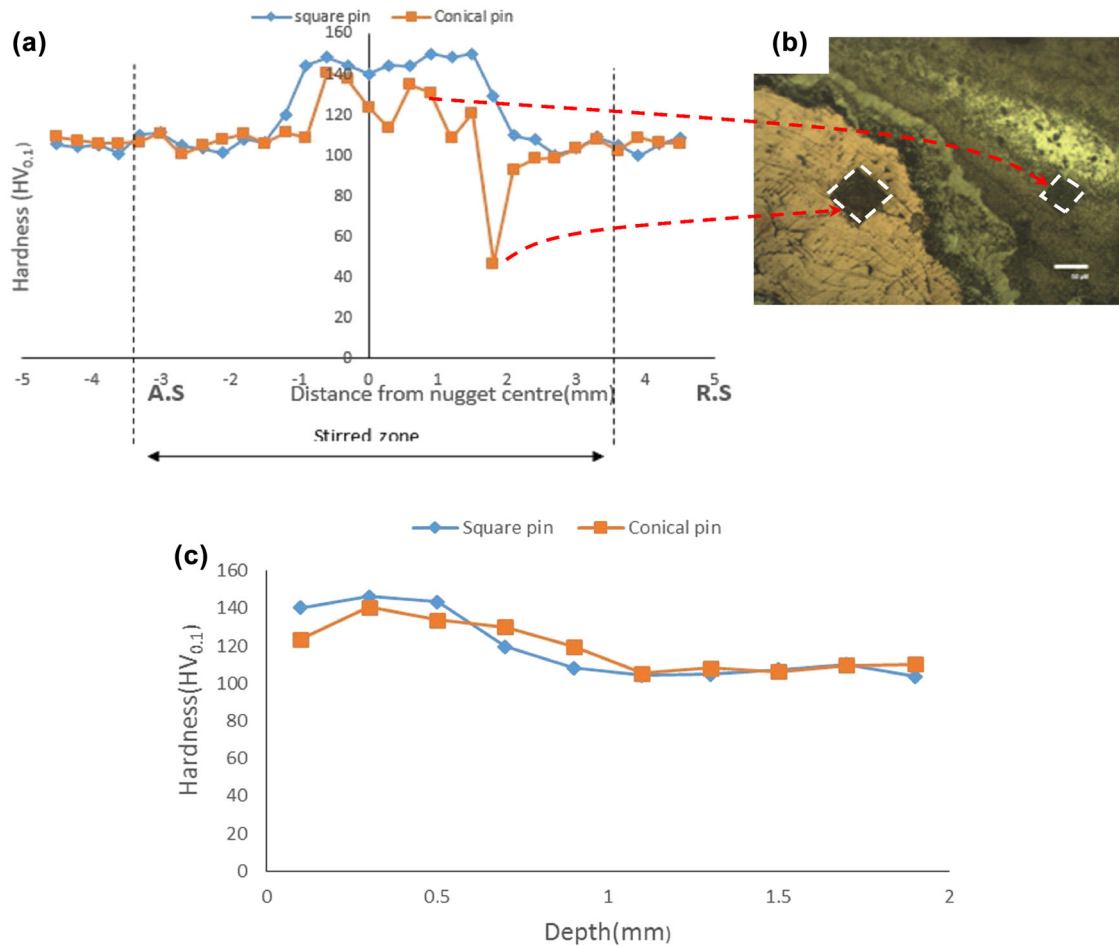


**Fig. 12** Microhardness distance profiles across the stirred zone (nugget zone) of FSSPed and age hardened Al 6061-Cu specimens (Cu spraying on 3 mm width and 1 mm deep groove) at various rotational speeds of tools—**a** 1300 rpm, **d** 2000 rpm, and **f** 3000 rpm. Microhardness depth profiles along the cross-section of the stirred zone at various rotational speeds of tools—**c** 1300 rpm, **e** 2000 rpm, and **g** 3000 rpm. **b** Micrograph of the region mentioned in (a). (A.S., advancing side; R.S., retreating side; sp, square pin tool and cp, conical pin tool)

the substrate after age hardening treatment (Figs. 12, 13). Surface alloying with Cu helps in the precipitation of Al<sub>2</sub>Cu phase (along with Mg<sub>2</sub>Si precipitates) in the surface alloyed stirred zone during the age hardening treatment.

#### 4 Conclusions

- Macroscopic defects in the stirred zone of Al 6061 were dependent on the friction stir surface processing (FSSP) parameters. Defects were not observed when the rota-

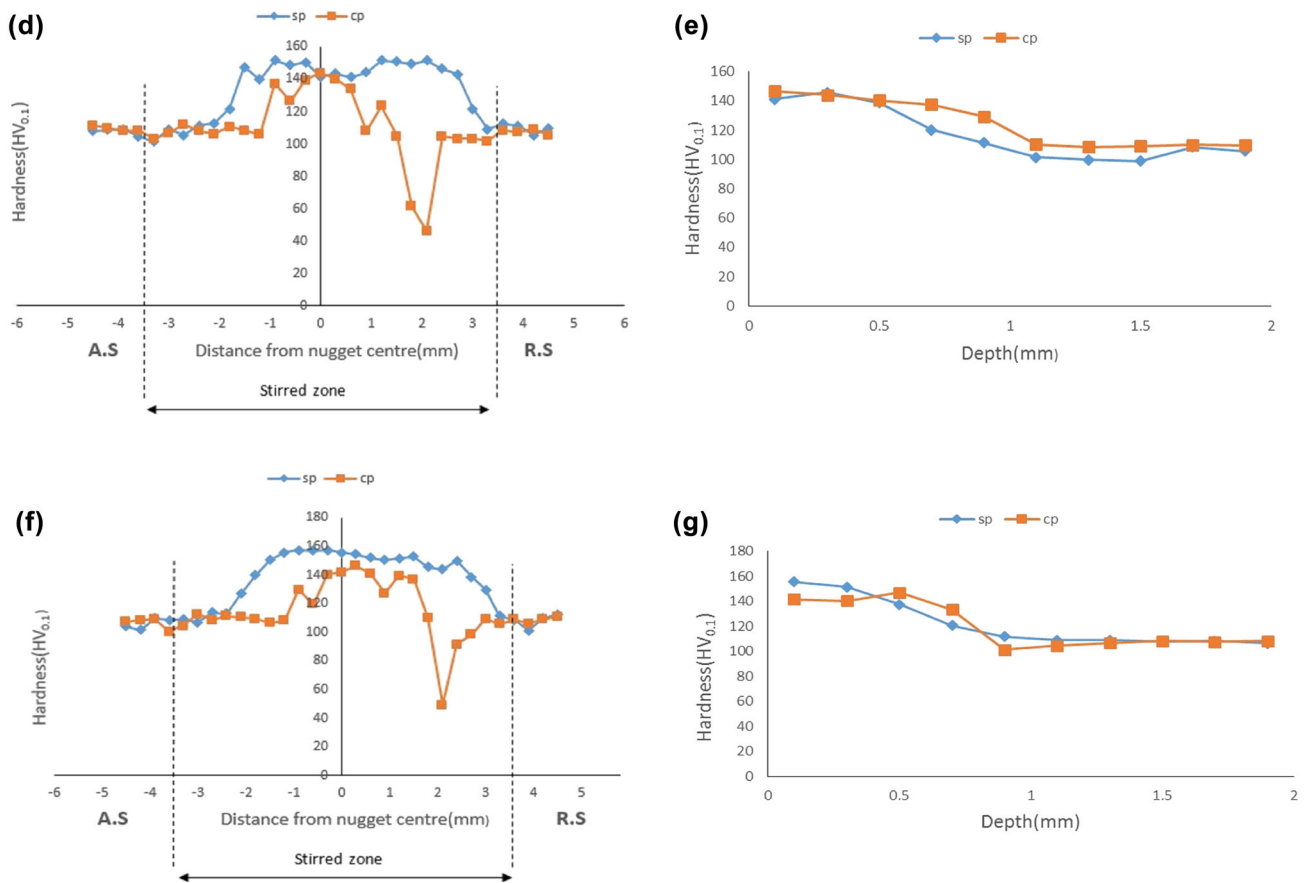


Fig. 12 continued

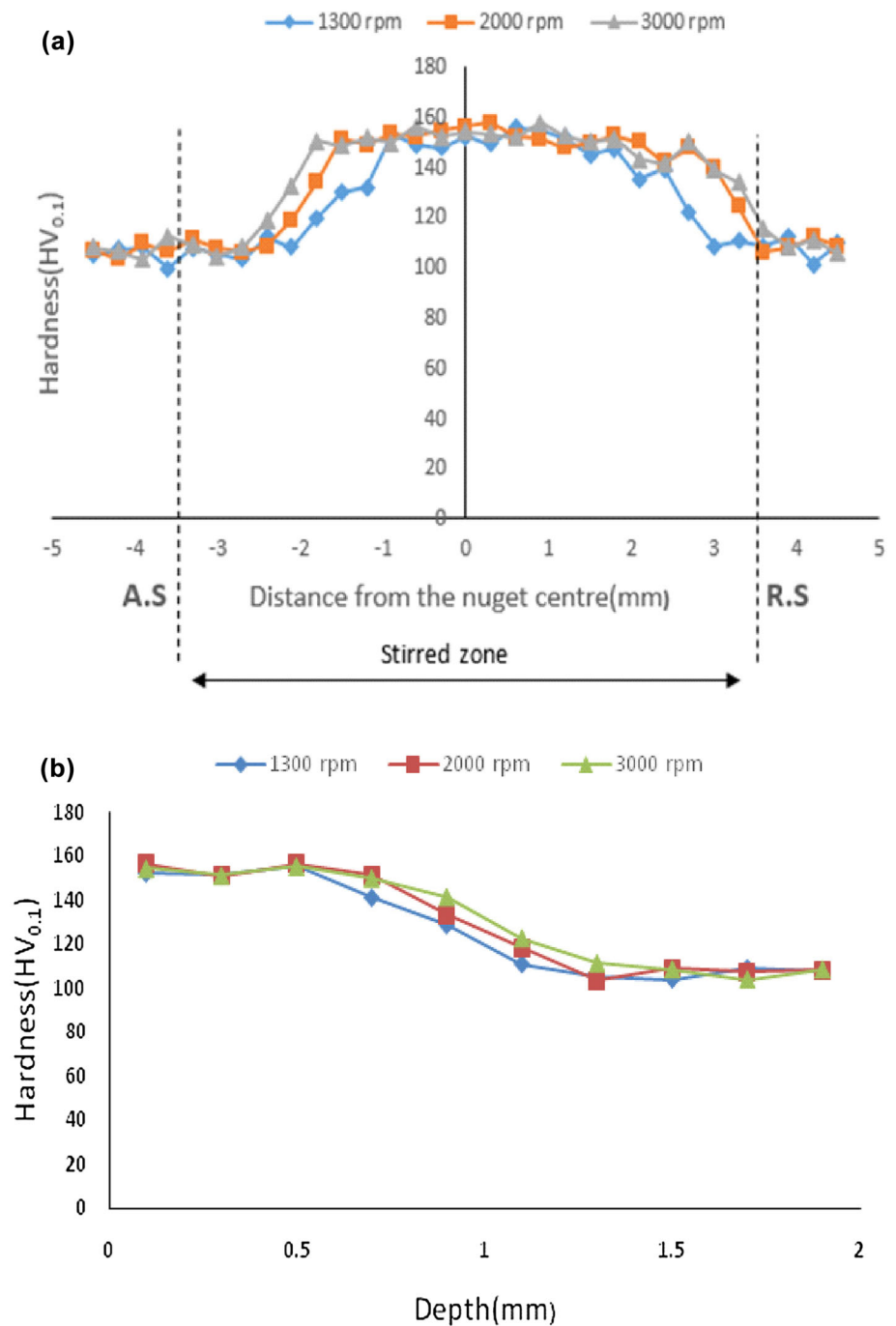
tional speed of the square and conical pin tools was increased from 1300 to 3000 rpm. At lower transverse speed (10 mm/min), defect-free stirred zone was observed. Increase in the traverse speed resulted in the poor mixing of the material.

- Friction stir surface processing (FSSP) was effectively used as a tool for solid state surface alloying of Al 6061 aluminium alloy using copper as the alloying element. Surface alloying followed by T6 heat-treatment resulted in considerable increase in the surface-hard-

ness of the stirred zone. This hardness of the stirred zone was 1.4 times the core hardness. FSSP enhanced the aging kinetics.

- Hardness profiles across the stirred zone were uniform and wider using square pin tool. Grain refining was observed in the stirred zone. The width of the hardness profile across the stirred zone was increased considerably with the increase in the rotational speed of the square pin tool.

**Fig. 13** **a** Microhardness distance profiles across the stirred zone of FSSPed and age hardened Al 6061-Cu specimens (Cu spraying on 5 mm width and 1 mm deep groove) FSSPed, using square pin tool at 10 mm/min transverse speed and with rotational speeds of 1300, 2000, and 3000 rpm. **b** Microhardness depth profiles across the cross-section of the stirred zone at various rotational speeds of tools—1300, 2000, and 3000 rpm



**Acknowledgements** Authors would like to thank the Department of Production Engineering and Industrial Management, COEP, for their cooperation during friction stir surface processing. Thermal-spray facility created at COEP through SERB Young Scientist Project (No. SR/FTP/ETA-52/2012—P.I.: Dr. Santosh S. Hosmani) is kindly acknowledged.

## References

1. Qu J, Xu H, Feng Z, Frederick D A, An L, and Heinrich H, *Wear* **271** (2011) 1940.
2. Mishra R S, and Ma Z Y, *Mater Sci Eng R* **50** (2005) 1.
3. Mahmoud E R I, Takahashi M, Shibayanagi T, and Ikeuchi K, *Wear* **268** (2010) 1111.
4. Gandra J, Mirandaa R, Vila P, Velhinho A, and Teixeira J P, *J Mater Process Technol* **211** (2011) 1659.
5. Mazaheri Y, Karimzadeh F, and Enayati M H, *J Mater Process Technol* **211** (2011) 1614.

6. Sharma V, Prakash U, and Manoj Kumar B V, *J Mater Process Technol* **224** (2015) 117.
7. Elangovan K, and Balasubramanian V, *Mater Sci Eng A* **459** (2007) 7.
8. Karthikeyan L, Senthilkumar V S, and Padmanabhan K A, *Mater Des* **31** (2010) 761.
9. Kurt A, Uygur I, and Cete E, *J Mater Process Technol* **211** (2011) 313.
10. Hofmann D C, and Vecchio K S, *Mater Sci Eng A* **402** (2005) 234.
11. Darras B, and Kishta E, *Mater Des* **47** (2013) 133.
12. Morisada Y, Fujii H, Nagaoka T, Nogi K, and Fukusumi M, *Compos A* **38** (2007) 2097.
13. Devaraju A, Kumar A, and Kotiveerachari B, *Mater Des* **45** (2013) 576.
14. Gandra J, Krohn H, Miranda R M, Vilaça P, Quintino L, and Santos J F, *J Mater Process Technol* **214** (2014) 1062.
15. Priyadarshini G S, Subramanian R, Murugan N, and Sathiskumar R, *Mater Manuf Processes* **32** (2017) 1416.
16. Patel V, Badheka V, and Kumar A, *Mater Manuf Processes* **31** (2015) 1573.
17. Sharma V, Gupta Y, Kumar V M, and Prakash U, *Mater Manuf Processes* **31** (2016) 1384.
18. Thankachan T, Soorya Prakash K, and Kavimani V, *Mater Manuf Processes* **33** (2018) 299.
19. Yuvaraj N, Aravindan S, and Vipin R S, *Trans Indian Inst Metals* **70** (2017) 1111.
20. Kim J, Hwang J, Kim H, Lee S, Jung W, and Byeon J, *Arch Metall Mater* **62** (2017) 1039.
21. Sakai T, Belyakov A, Kaibyshev R, Miura H, and Jonas J J, *Prog Mater Sci* **60** (2014) 130.
22. Porter D A, and Easterling K E, *Phase Transformations in Metals and Alloys*, Chapman & Hall, London (1981).
23. Courtney T H, *Mechanical Behavior of Materials*, Waveland Press Inc, Illinois (2005).
24. ASM International, *ASM Handbook 2. Properties and Selection: Nonferrous Alloys and Special-Purpose Materials*, ASM International, Materials Park, OH (1992).
25. Thomas W M, and Nicholas E D, *Mater Des* **18** (1997) 269.